


Light emission at reverse voltage in a wide-well (In, Ga)N/GaN light-emitting diode

Artem Bercha¹, Konrad Sakowski^{1,2}, Grzegorz Muziol¹, Mateusz Hajdel¹ and Witold Trzeciakowski^{1,*}

¹*Institute of High Pressure Physics, Polish Academy of Sciences, Sokolowska 29/37, 01-142 Warsaw, Poland*

²*Institute of Applied Mathematics and Mechanics, University of Warsaw, Banacha 2, 02-097 Warsaw, Poland*

 (Received 14 December 2023; revised 15 March 2024; accepted 30 April 2024; published 15 May 2024)

This study examines the effects of negative voltage pulses (NVPs) on emission from (In, Ga)N/GaN light-emitting diodes (LEDs) with a wide quantum well in the active layer. For low dc forward voltages (1–3 V), the diode emits light only during the periodic application of the NVPs, provided that the separation of NVPs is sufficiently large (from a few microseconds to milliseconds). These effects are due to a slow buildup of “dark charge,” i.e., charge in the ground state of the wide well. The NVPs reduce the electric field in the well and deplete dark charge from the well (through radiative and nonradiative recombination). After the NVP, the concentration of dark charge once again slowly increases and saturates. For low forward voltages (or currents), the saturation occurs after milliseconds, which is caused by the long buildup times of dark charge. By varying the duration of NVPs, we can estimate the decay time of dark charge for a given negative voltage. This decay time decreases rapidly with increasing (absolute value of) negative voltage. We present a numerical model of LED emission, which is in qualitative agreement with experimental results. Short pulses of light generated by NVPs may create new applications for wide-well LEDs and laser diodes.

DOI: [10.1103/PhysRevApplied.21.054030](https://doi.org/10.1103/PhysRevApplied.21.054030)

I. INTRODUCTION

(InGa)N/GaN Light Emitting Diodes (LEDs) are typically grown via a metal-organic vapor-phase epitaxy on a (0001)-plane of GaN. Quantum wells (QWs) in the active layer of these structures suffer from strong built-in fields, which are detrimental to the radiative efficiency of the LEDs [1–3] since they reduce the overlap of electron and hole wave functions in the well. These fields can be reduced by the opposing field of the p-n junction of the diode and by the reverse voltage applied to the LEDs [4–6]. Since the overlap decreases with increasing well width [7,8], commercial LEDs employ narrow quantum wells (2–3 nm wide). However, it was also found [9] that the electric field in the well can be substantially reduced by free carriers injected into the well (by illumination or by a forward current). Reference [9] also demonstrated that, even for very high concentrations of injected electrons and holes, the ground states of both carriers remain localized close to the edges of the well. This means that, in very wide wells (10–25 nm), the charge in the ground states will be very effective in screening the built-in field, but it will not contribute to radiative recombination [10]. Interestingly, it was found that screening of the electric field facilitates

emission via excited states which extend over the whole well [11–15]. Charge in the ground states (which we call “dark charge”) has very long (millisecond) lifetimes, while charge in the excited states decays in nanoseconds and gives rise to strong light emission (as soon as the electric field is screened). Wide quantum wells have been used as active regions in both light-emitting diodes [11–14] and laser diodes [15–17]. These structures (usually grown by molecular-beam epitaxy) were used for research purposes, not in commercial devices. The screening of the electric field is predicted to improve the efficiency of (InGa)N LEDs based on wide wells [11]. Furthermore, due to effective screening and radiative transitions via excited states, the emission wavelength does not change with current density [13]. This is in stark contrast to narrow-well LEDs, in which the emission wavelength blueshifts in a wide range [13,15]. Another interesting aspect of wide (In, Ga)N/GaN quantum wells is the transition from a two- to a three-dimensional system as the electric field is reduced [18].

Since the built-in field in Ga-polar (In, Ga)N/GaN quantum well is opposed to the field generated by the p-n junction in LEDs, the application of negative (reverse) voltage reduces the electric field in the quantum well and facilitates the optical emission, contrary to standard GaAs or InP LEDs or nonpolar GaN LEDs where the reverse

*Corresponding author: wt@unipress.waw.pl

voltage increases the field in the well. This occurs both for narrow [19,20] and for wide wells [21]. Such emissions have been studied in time-resolved electroluminescence measurements in the nanosecond time range, characteristic of excited-state emission [21]. The idea here was to pump the well at a positive voltage and generate the emission at a negative voltage. As the emission at the negative voltage occurs at a reduced electric field, it should be more intense; it has been proposed as a way to improve the efficiency of commercial LEDs [20].

Interestingly, dark charge can be studied through its screening and band-filling effect, which modifies the emission via excited states [22–25]. Photocurrent measurements of wide-well LEDs revealed an anomalous (forward) direction for the photocurrent and a strong dependence on chopper frequency [22], which indicated slow changes for the electric field in the well. This motivated time-resolved studies of wide-well LEDs in the microsecond to millisecond range. In Ref. [23], we compared photoluminescence (PL) from wide and narrow wells under pulsed excitation. A slow increase of PL in wide wells and their dependence on the excitation period was related to filling the ground states with charge before the excited states could be populated. We studied the influence of negative voltage pulses (NVPs) on PL and outlined a simple theoretical model that agreed qualitatively with observed effects. In Ref. [24], the time-resolved PL from wide wells showed nanosecond decay times for excited-state transitions. This was in contrast to the microsecond to millisecond decay of ground-state transitions, revealed by a slow decay of the short pulses of light (SPLs) accompanying NVPs. Finally, in our recent paper [25], we performed a systematic study of the decay of PL as a function of the excitation period; it was revealed that dark charge persists in the quantum well up to 30 ms after photoexcitation. The NVPs were found to deplete dark charge from the quantum well, so that after the NVP the concentration of dark charge increases slowly toward some equilibrium value (dependent on the Fermi level position with respect to the quantum-well edges). It was determined that the reverse voltage reduces the decay and regeneration times of dark charge, since it reduces the electric field in the well.

In the present paper, we perform electroluminescence (EL) measurements on wide-well LEDs in a scheme in which the light emission occurs only at a negative voltage. This is exclusively possible due to the extremely high built-in electric field present in the wide quantum well in the equilibrium state. An LED is pumped by a low forward current that fills the quantum well. No detectable emission is observed, but the electric field becomes lower. When an NVP is applied, a bright emission appears as a short (20–30 ns) SPL at the leading edge of the NVP. The intensity of these SPLs depends on the concentration of dark charge; by varying the duration and value of the forward current pumping the well and the duration and voltage of

the NVP, we can gain insights into the concentration of dark charge. Our method is similar to the studies of commercial LEDs in Ref. [20]; the authors of this work studied narrow (InGa)N quantum wells, which also emitted light at a forward bias. In the present paper, we exploit the lack of emission from the wide well at a positive voltage and achieve bright emission at a negative voltage.

Short pulses of light at a reverse voltage could be attractive both for pulsed LEDs and for pulsed laser diodes since they do not require sophisticated pulse generators, only a fast change of voltage. In the case of laser diodes with wide wells, it is possible to pump a high concentration of spatially separated electrons and holes (due to a large field) and a rapid change of voltage (a reduction of the field) could lead to a high population inversion, i.e., a high gain. In the presence of stimulated emission in a laser structure, the SPLs should be much shorter (than in LEDs) and more intense. The possibility of achieving lasing during the application of the NVPs is discussed in a separate section. Finally, the slow decay of charge in wide-well LEDs creates the possibility for its use as a charge-coupled device.

Furthermore, in the present paper, we construct a simplified model to understand the accumulation of dark charge with a positive bias and the conditions for the appearance and saturation of SPLs. We also perform numerical simulations within a drift-diffusion model, which complements the experimental procedures. This helps us attain insights into optimizing the emitters for generating strong SPLs (for pulsed laser applications).

II. SAMPLES AND EXPERIMENT

Our LED samples (with a 25-nm quantum well) are schematically shown in Fig. 1(a). They were grown by plasma-assisted molecular-beam epitaxy (PAMBE) on bulk Ga-polar c-plane n-GaN substrates. The layers of the LED were as follows: 100-nm n-GaN:Si (Si: $2 \times 10^{18} \text{ cm}^{-3}$), 40-nm-thick $\text{In}_{0.02}\text{Ga}_{0.98}\text{N}$ lower barrier, 25-nm $\text{In}_{0.17}\text{Ga}_{0.83}\text{N}$ well, 20-nm $\text{In}_{0.02}\text{Ga}_{0.98}\text{N}$ upper barrier, p- $\text{Al}_{0.13}\text{Ga}_{0.87}\text{N}:\text{Mg}$ (Mg: $2 \times 10^{19} \text{ cm}^{-3}$) electron blocking layer (EBL), and 200-nm p-GaN:Mg (Mg: $5 \times 10^{18} \text{ cm}^{-3}$). Next, an (In,Ga)N tunnel junction was grown and capped with a 100-nm n-type GaN:Si on top. The metal contacts formed a rectangular frame on the upper surface, enabling us to study the emission from the diode (or illuminate it) through the opening in metalization. The area of the active region of our diodes was approximately $0.3 \times 0.3 \text{ mm}^2$. We verified (by cathodoluminescence) that no trace of dislocations was found in similar $\text{In}_{0.17}\text{Ga}_{0.83}\text{N}$ layers up to a thickness of 40 nm. Therefore, there should be no relaxation in our quantum wells.

The diode was operated under forward voltage from +1 to +3 V and NVPs were applied periodically from a

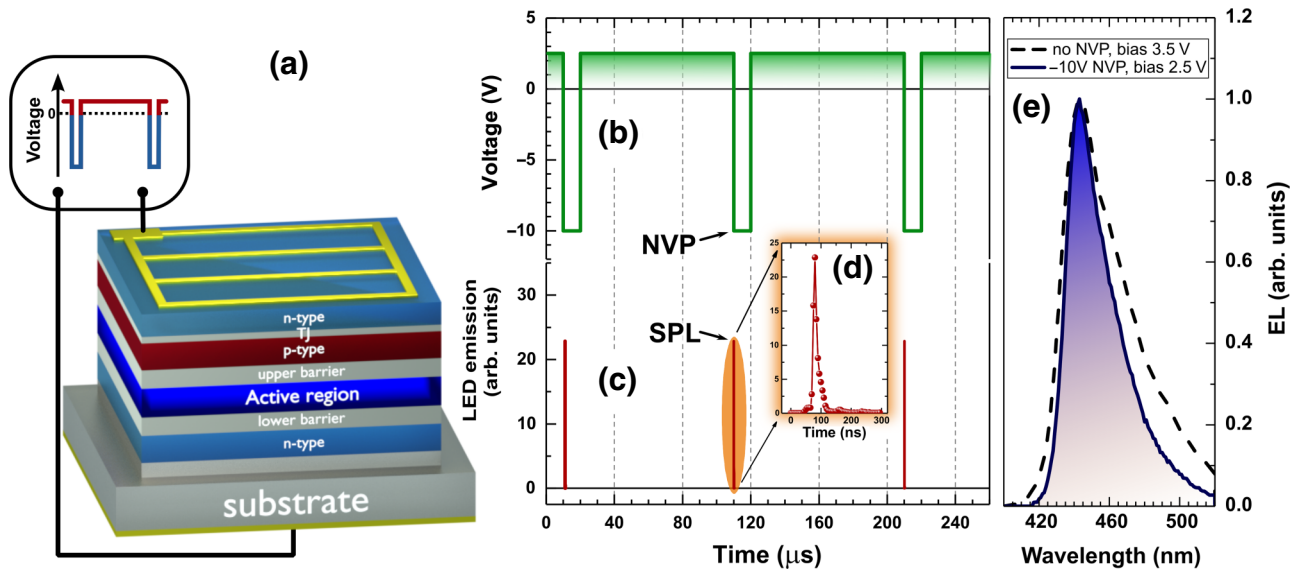


FIG. 1. (a) Schematic structure of the LED, (b) voltage applied to the diode, (c) emission intensity from the LED as a function of time (for forward voltage of +2.5 V and the period of NVPs equal to 100 μ s), (d) magnified SPL intensity versus time, and (e) normalized emission spectrum of SPL at -10 V (solid line) and the normalized electroluminescence (EL) spectrum of LED at 3.5 V (dashed line).

pulse generator; we used -10 , -5 , and -3 V pulses lasting for 0.1 μ s to 10 ms. The temporal separation of the NVPs was increased from 1 μ s to 10 ms. During this time, the charge is pumped into the well until the arrival of the next NVP. The emission from the LED was recorded by a Spex1000M monochromator and a photomultiplier with photon counting. This detector had a time resolution of 5 ns, but we were mainly studying slower processes in the microsecond to millisecond range. All our experiments were performed at room temperature.

III. EXPERIMENTAL RESULTS

The current captured by the quantum well is the most important quantity affecting the concentration of charge in the well. However, for low voltages applied to the diode (1–3 V), the shunt (parallel) conductivity of our diodes dominates the I – V , and the current flowing through the quantum well is orders of magnitude lower than the total (measured) current. Therefore, in the following, we label our results with voltages instead of currents.

Figure 1 shows the basics of the experiment: (a) LED structure, (b) voltage applied to the diode, and (c) emission intensity of the diode as a function of time. Short pulses of light (SPLs) appear at the leading edges of the NVPs. The diode is operated at a forward voltage [+2.5 V in Fig. 1(b)] and the NVPs [-10 V for 10 μ s] are applied periodically [every 100 μ s in Fig. 1(b)]. Since the intensity of an individual SPL is low, we added the intensity of 1000 subsequent SPLs in each case. In Fig. 1(d), we show the example of an SPL measured with 5 ns resolution. The SPLs had 10–20 ns width (at half maximum). Figure 1(e)

shows the spectrum of the SPL emission. This spectrum is almost the same as the electroluminescence spectrum at higher forward voltages since both are due to transitions between excited states while the electric field is screened. The SPL emission occurs at a negative bias (-10 V) while electroluminescence from the diode occurs at a positive bias (+3.5 V), but the emission spectrum from the wide wells does not shift with voltage due to efficient screening, as shown in several previous papers [15,23,25]. When the negative (reverse) voltage is applied to the diode, the electric field in the (unscreened) well is reduced [25,26]. Therefore, the energetic distance between the ground and excited states is also reduced. Here, less charge is needed to screen the field and some portion of dark charge is “promoted” to the excited states, which recombine (radiatively and nonradiatively) since their electron-hole wave function overlap is higher (this is illustrated later in Figs. 7 and 8 of Sec. V). Dark charge is depleted during each NVP and increases until the next NVP. It is, therefore, both the forward current flowing through the LED and the separation of NVPs that are important for the buildup of dark charge (period minus NVP duration). In Fig. 1(b), the period is 100 μ s and the separation of NVPs is 90 μ s. It is interesting that relatively short (20 ns) pulses of light can be generated by switching to a negative voltage.

A similar method of periodic NVPs was applied to commercial diodes (with narrow wells) in Ref. [20], where the charge in the ground state recombines radiatively. The decay times were in the range of tens of nanoseconds. The duration of the NVPs, as well as their period, was fixed in Ref. [20]; in our study on wide-well LEDs, these parameters are varied in order to reveal a slow buildup of dark

charge during the application of forward voltage and its decay during the application of reverse voltage. There is a strong wavelength shift (with voltage) in narrow wells, while the emission wavelength is stable in wide wells due to effective screening (and due to the fact that excited-state transitions are less sensitive to the electric field than ground-state transitions).

In our experiment, the separation between subsequent NVPs is increased (from 1 μ s up to 10 ms) so that the charging time of the well is increased, and we measure the integrated intensity of the SPLs as a function of this separation (for several forward voltages), see Fig. 2(a). For low voltages up to 1.25 V, there is no measurable emission from the sample. At 1.4 V, the SPLs start to appear if the separation of NVPs (charging time) is over 1 ms. For increasing voltage (or current), this “threshold separation” is reduced. Above the “threshold separation,” the intensity of SPLs increases and saturates. The saturation intensity of SPLs increases with forward voltage (or current). This is very different from SPLs in narrow-well LEDs [20]. In our studies, there is no emission in between the NVPs (due to a low forward voltage), while the SPLs are only observed in narrow wells when the LED opens up (at a higher forward voltage).

The NVPs deplete dark charge from the quantum well (partially or completely, depending on their voltage and duration). If their separation is short, dark charge does not sufficiently recover when the next NVP arrives and emission (SPL) is absent. If the separation of the NVPs is sufficiently long and the current that pumps the well is adequate, the emission appears at the beginning (leading edge) of each NVP.

We performed the same experiment for reduced negative voltage during the NVP: -5 V [Fig. 2(b)] and -3 V [Fig. 2(c)]. For a reduced negative voltage, the SPL intensities are much lower and appear for longer NVP separations (i.e., for higher concentrations of dark charge). This is consistent with the fact that, for wide (In,Ga)N/GaN wells, the PL emission increases with increased negative voltage [25] (i.e., a reduced electric field in the well). Apparently, since the SPL intensity is lower for a reduced NVP voltage, we need a higher dark charge concentration to observe SPLs, so they appear after longer charging times.

From the above results, we can determine the threshold separation t_{th} at which the SPLs appear and the saturation separation t_{sat} above which the intensity of the SPLs saturates. These two quantities can be interpreted as the time after which the dark charge exceeds some threshold value n_{th} and the time after which it saturates. Both of these times decrease approximately exponentially with an increasing forward voltage (Fig. 3). This is due to the fact that the charging current increases exponentially with voltage. The errors are large, especially for the saturation times, but the trend can be clearly observed.

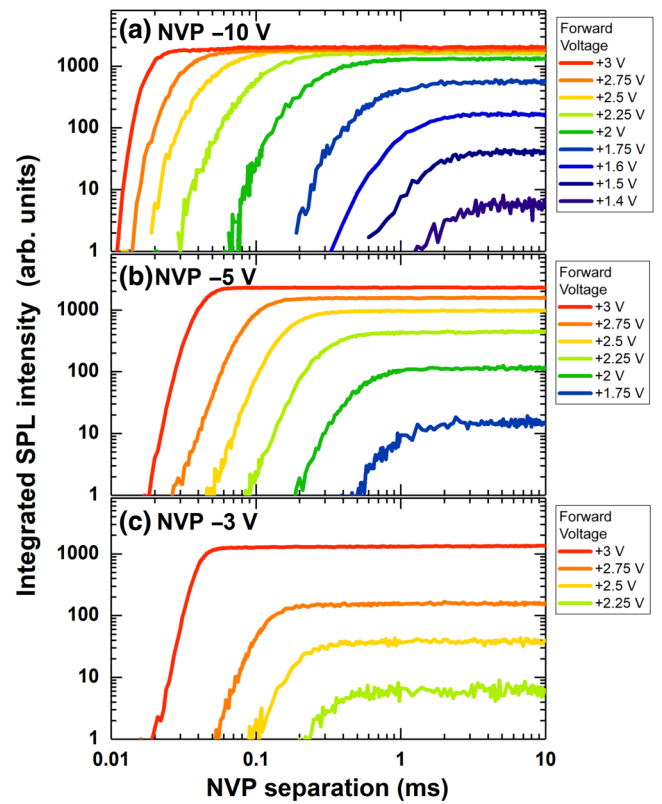


FIG. 2. Integrated intensity of the SPLs as a function of the separation of 10- μ s NVPs for different forward voltages applied to the LED and three values of negative NVP voltage: (a) -10 V, (b) -5 V, and (c) -3 V. SPLs appear at some threshold separations of the NVPs and saturate. They increase for growing forward voltages (or currents) between NVPs and for increased negative voltages during NVPs.

Next, we examined how the duration of the NVPs affects the curves in Fig. 2 (i.e., the intensity of the SPLs versus the NVP separation). This allows us to estimate the decay time of dark charge in the well at a given negative voltage (during the NVP). When the NVP is sufficiently long, the concentration of dark charge should drop to low values, and a further increase in the NVP duration should not change the buildup of dark charge with a positive voltage until the next NVP arrives (i.e., the SPL intensities versus charging time should not change anymore). The relaxation of dark charge has been measured in Ref. [25] through the decay of PL pulses [Fig. 13(c) in Ref. [25]] at negative voltages down to -4 V. Here, we apply negative voltages of -10 , -5 , and -3 V, using SPL intensity (versus charging time) as an “indicator” of dark charge. The dependence of SPL intensity on charging time is shown in Fig. 4 for the forward voltage of 2.5 V, three values of NVP voltage, and six NVP durations. We can see that the saturation of SPLs as a function of NVP separation occurs for much longer durations of NVPs when we reduce the negative voltage. For example, with a -10 V bias, the curves saturate at an

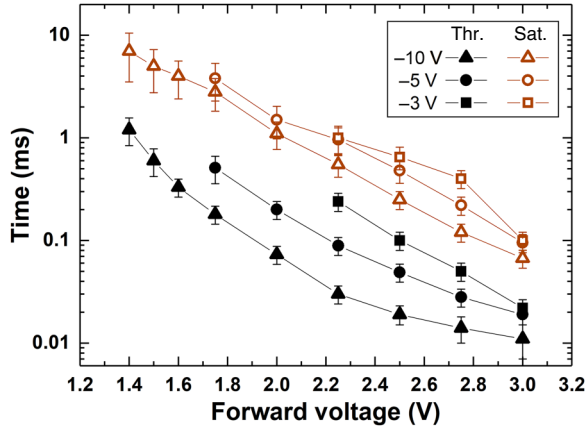


FIG. 3. Separation of the NVPs (charging time) when SPLs start to appear (black solid symbols represent threshold time, t_{th}) and when its intensity saturates (red hollow symbols depict saturation time, t_{sat}) as a function of the positive applied voltage to the LED (for NVP voltages of -10 , -5 , and -3 V, and an NVP duration of $10 \mu\text{s}$). These times are determined from Figs. 2(a)–2(c).

NVP duration of about $10 \mu\text{s}$. With a -5 V bias, this happens around $100 \mu\text{s}$ and, with a -3 V bias, we have not observed saturation up to 1 ms.

It is interesting to note that the SPL is not present for the whole duration of the NVP since it only appears at the leading edge of the NVP, as shown in Fig. 1. Therefore, the observed dependence of the SPL on the duration of the NVP, presented in Fig. 4, implies that there are nonradiative slow processes present, which contribute to a reduction in dark charge.

In Fig. 5, we plot the threshold time (the charging time when the SPLs appear in Fig. 4) versus the NVP duration. In Fig. 4, we show only curves for six NVP durations (for clarity) but, in Fig. 5, we show more experimental points (the error bars were estimated from the “wiggles” in Fig. 4 to be around 20% of the corresponding threshold times). The saturation of threshold time indicates that the well has been almost fully depleted from dark charge during the NVP. The reduction of negative voltage increases the electric field in the well, which slows down the decay of dark charge and, therefore, requires longer NVP durations to achieve full depletion. This is consistent with Fig. 13(c) in Ref. [25] if we remember that saturation occurs after 3 to 4 relaxation times.

IV. SIMPLE INTERPRETATION

We have shown in Ref. [25] that dark charge can be present in wide quantum wells without any external excitation. This happens when the potential drop in the empty well exceeds the value of the bandgap. We denote the concentration of this charge by n_{eq} . It depends on the position of the edges of the well with respect to the Fermi level, so it may be different for electrons and holes. It

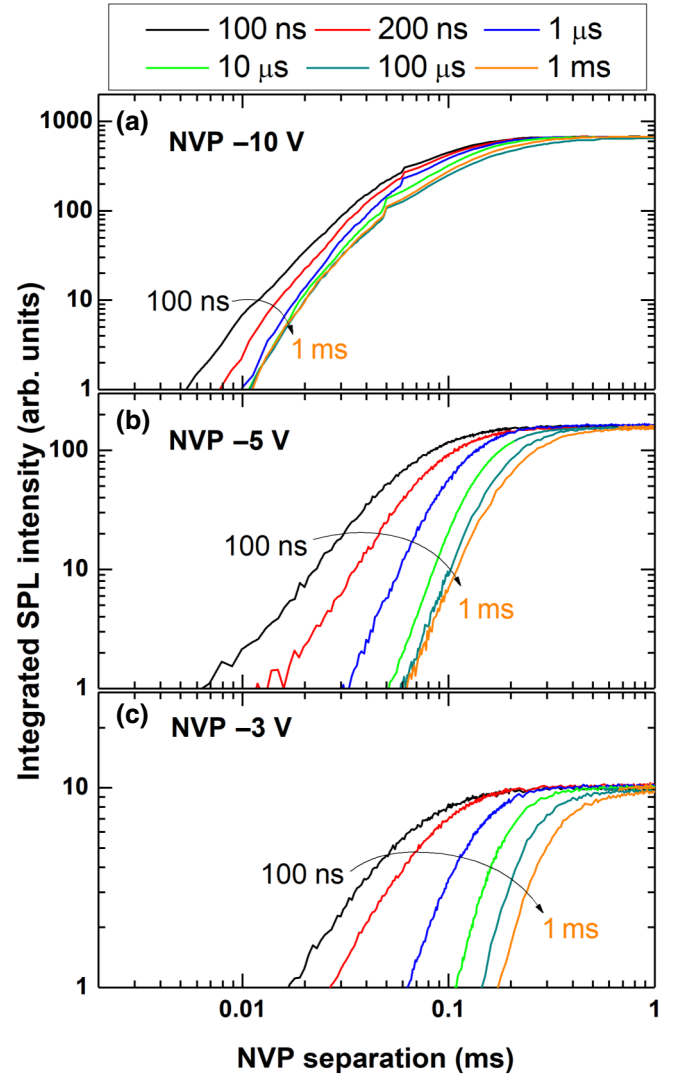


FIG. 4. SPL intensity as a function of NVP separation (charging time) for three different values of negative applied voltage during an NVP: (a) -10 V, (b) -5 V, and (c) -3 V and for increasing duration of the NVP (from 100 ns to 1 ms). Here, the forward voltage applied to the LED is 2.5 V and only the parameters of the NVP (voltage and duration) vary. When the NVP duration is sufficiently long, dark charge is depleted during the NVP and the SPL intensity versus charging time stabilizes.

can be depleted by the application of the NVP and then it increases (regenerates) toward n_{eq} . If the diode is biased and the current density is j , a fraction α of this current will be trapped by the well. Therefore, the concentration of dark charge n will be governed by the simple equation

$$\frac{dn}{dt} = -\frac{n - n_{eq}}{\tau} + \frac{\alpha j}{e}, \quad (1)$$

where e is the electron charge and τ is the relaxation time of dark charge. In Ref. [25], we found that τ was of the order of milliseconds (at a voltage of zero) and that it was similar for both decay ($n > n_{eq}$) and regeneration ($n < n_{eq}$).

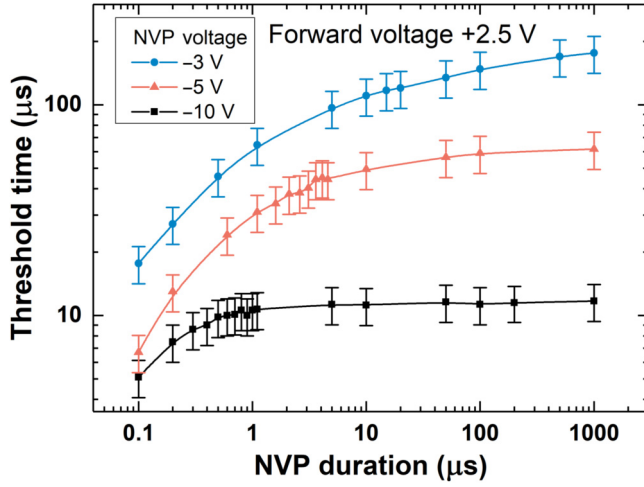


FIG. 5. Threshold time (charging time when SPLs appear) versus NVP duration (obtained from Fig. 4 and for more NVP durations) for three different values of the NVP voltage. Saturation of the threshold time indicates that dark charge is depleted during the NVP and a further increase in the NVP duration does not change the SPL emission.

It decreased under reverse bias applied to the diode, i.e., it dropped with a decreasing field in the well. This means that, in the presence of current j pumping the well, the relaxation time will be longer when the well is empty (i.e., right after the NVP), but it will be much shorter when the well is filled with carriers and the field is screened. Therefore, Eq. (1) is a very crude approximation, in which τ is some average relaxation time that can be expected to decrease with increasing j . We observed this in Ref. [25] when the decay of dark charge was much faster straight after optical excitation and slower after a longer time.

The solution of Eq. (1) is as follows:

$$n(t) = \left[n(0) - n_{\text{eq}} - \frac{\alpha j \tau}{e} \right] \exp\left(-\frac{t}{\tau}\right) + n_{\text{eq}} + \frac{\alpha j \tau}{e}, \quad (2)$$

which shows that, for $t \gg \tau$, the concentration saturates at the value $(n_{\text{eq}} + (\alpha j \tau / e))$. As a graphical illustration in Fig. 6, assuming $n(0) = 0$ and $n_{\text{eq}} = 1 \times 10^{12} \text{ cm}^{-2}$, we plot $n(t)$ for three values of αj : 1, 3, and 5 mA/cm^2 , and for the corresponding values of τ : 0.5, 0.3, and 0.2 ms. If we assume the threshold concentration of dark charge as $n_{\text{th}} = 5 \times 10^{12} \text{ cm}^{-2}$, we can see that the threshold concentration is not achieved for the lowest current (1 mA/cm^2), so we should not observe SPLs in this case. For an increasing current, the threshold concentration is achieved after a shorter “charging time” t_{th} (marked by black arrows in Fig. 6).

This is in qualitative agreement with our experimental results (Fig. 2). If the diode is under a low forward bias, then there is no SPL emission. However, when we increase the current and $n(t)$ exceeds some threshold value n_{th} ,

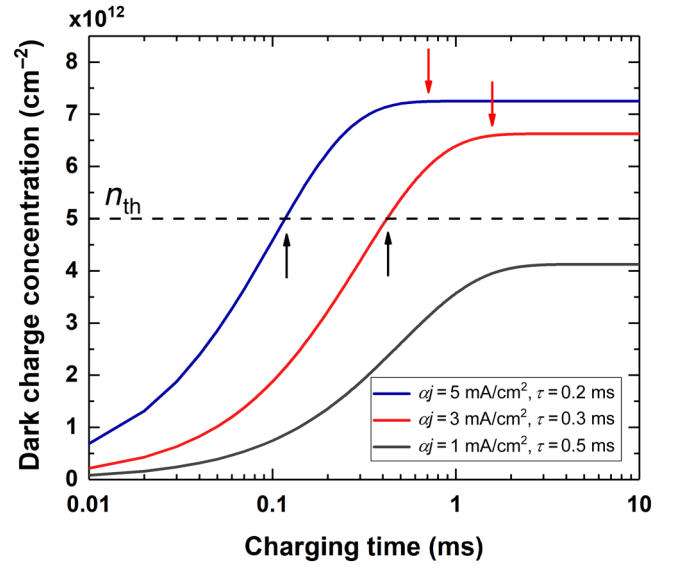


FIG. 6. Increasing concentration of dark charge [given by Eq. (2)] after depletion by the NVP for three different values of the current density. Black arrows denote the threshold times and red arrows indicate the saturation times. All the parameters are defined in the text.

the reduced electric field in the well during the NVP will lead to a population of excited states and short pulses of light. Our experimental results indicate that an NVP with a reverse voltage of -10 V and a duration of $10 \mu\text{s}$ depletes the dark charge effectively. However, at NVP voltages of -5 and -3 V , a longer NVP duration is needed to deplete dark charge from the well. According to data shown in Fig. 5, full depletion is achieved after $100 \mu\text{s}$ at -5 V , while we have not found saturation up to 1 ms for -3 V .

In our experiment, we cannot directly measure the concentration of dark charge but we can observe SPLs (due to excited-state emission) that appear when $n(t) \geq n_{\text{th}}$ and saturate for a charging time $t \gg \tau$. By increasing t (i.e., the separation between the NVPs), we can determine the time t_{th} needed to achieve n_{th} and estimate τ by determining the time needed to observe the saturation of light pulses.

The above-simplified picture is consistent with the experimental results, but a more complete analysis requires the time-dependent modeling of transport and recombination of wide-well LEDs, which is outlined in the next section.

V. NUMERICAL MODELING OF LED

For numerical simulations, we use a transient one-dimensional drift-diffusion model [27,28], which is often used in simulations of luminescent semiconductor devices. For the calculations, we use the numerical code PMICRO, which is proprietary software developed at the Institute of High Pressure Physics, Polish Academy

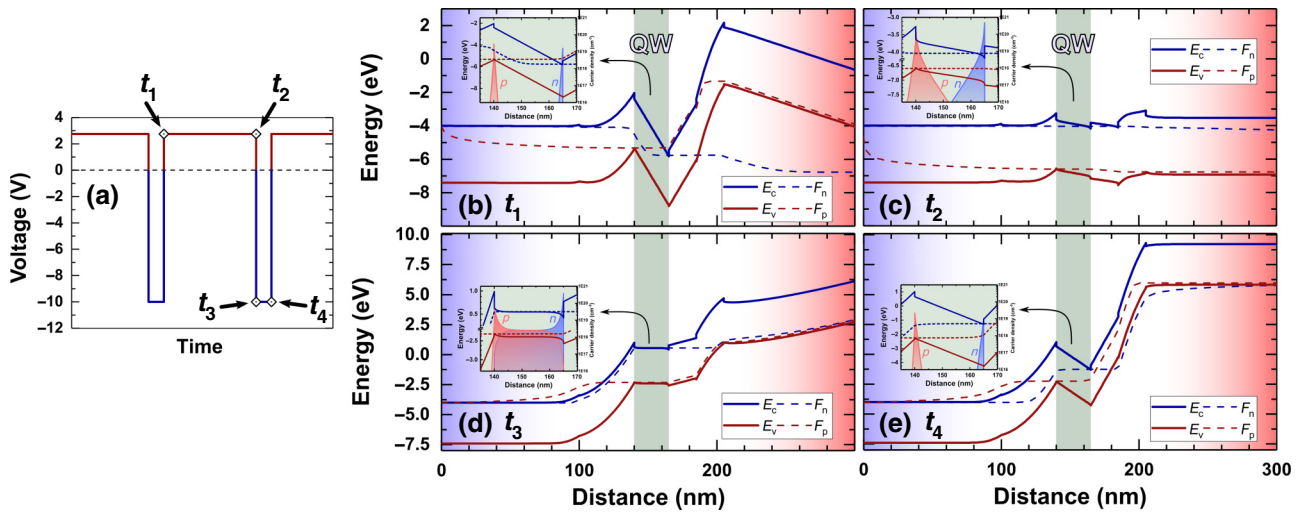


FIG. 7. Band diagrams for the LED at four different moments (t_1 , t_2 , t_3 , and t_4) of the periodic experimental procedure [marked in (a)]. Starting from the top left: (b) depleted well at 2.75 V, (c) charged well after 1.5 ms charging time at 2.75 V, (d) charged well just after application of the NVP at -10 V, and (e) discharged well at the end of the NVP pulse at -10 V. Quasi-Fermi levels are shown with dashed lines for electrons (blue) and holes (red). Expanded band diagrams in the quantum well (QW) region, together with electron and hole charge densities, are shown in the insets.

of Sciences [29]. The underlying differential equations of the model are discretized by the composite discontinuous Galerkin method [30,31] in space and with the implicit Euler method in time. The model accounts for the Shockley-Reed-Hall, radiative, and Auger recombination channels. We simulate the fragment of the original structure: 100-nm n-GaN:Si, 40-nm-thick $\text{In}_{0.02}\text{Ga}_{0.98}\text{N}$ lower

barrier, 25-nm $\text{In}_{0.17}\text{Ga}_{0.83}\text{N}$ well, 20-nm $\text{In}_{0.02}\text{Ga}_{0.98}\text{N}$ upper barrier, p- $\text{Al}_{0.13}\text{Ga}_{0.87}\text{N}:\text{Mg}$ EBL, and 200-nm p-GaN:Mg. The following tunneling junction is not included, as spatial tunneling between bands is not accounted for in the model. The goal of the simulations was to reproduce the qualitative aspects of the observed phenomena, not to attain the quantitative values.

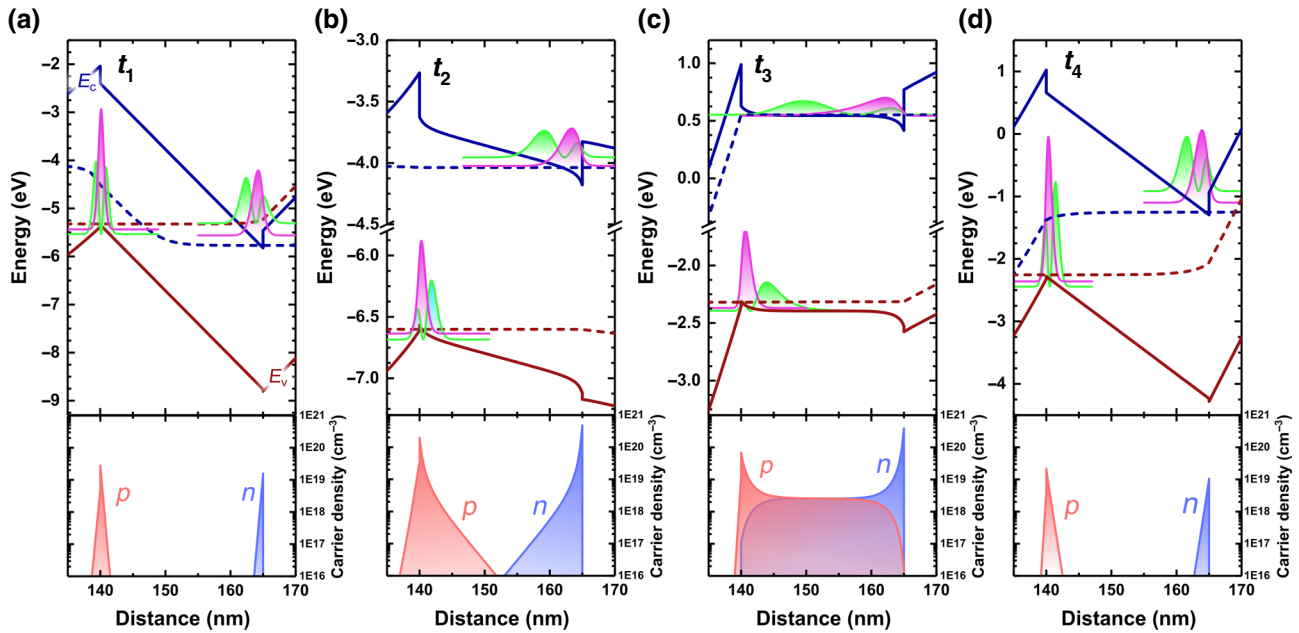


FIG. 8. Expanded band diagrams in the region of the quantum well at four different moments (t_1 , t_2 , t_3 , t_4) with the squares of wave functions of the two lowest states (for electrons and holes). Total electron and hole charge densities (in a logarithmic scale) are shown below each diagram.

Let us first show, in Fig. 7, the band diagrams obtained from the model for the four steps of the experimental procedure: (i) t_1 , straight after the NVP at a forward voltage of 2.75 V (charges depleted by the NVP), (ii) t_2 , well filled with dark charge after 1.5 ms of current flow at 2.75 V, (iii) t_3 , well with reduced electric field (due to the application of the NVP at -10 V), and (iv) t_4 , well at the end of the NVP after the charge has recombined at -10 V.

In Fig. 8, we show the magnified band diagrams in the quantum-well region, together with the squares of wave functions of the ground and the first excited states of the electrons and holes (and the total electron and hole charge densities in the well).

At moment t_1 (straight after the NVP, at a positive voltage of 2.75 V), the well contains very little charge, which is located close to its edges. Both wave functions (ground and excited states) for the electrons and holes show negligible overlap. It is important to note that the well is not in equilibrium because the carriers were depleted during the NVP. Therefore, during the time between t_1 and t_2 , the well is charged by a low-intensity current and the field becomes partly screened. The inflow of carriers is balanced by some occurrence of nonradiative recombination (Shockley-Read-Hall). The total current densities of the electrons and holes approach each other, but there is still no detectable emission from the well. Next, when we apply a negative voltage of -10 V (moment t_3), the field in the well is rapidly reduced (we assume that the change of voltage is much shorter than the recombination time of the carriers). The wave functions of electrons and holes spread into the well, but the ground states still have a very small overlap compared with the excited states. The excited states with high overlap generate short emission pulses (SPLs) followed by some occurrence of nonradiative recombination. The recombination during the NVP leads to a reduced charge density (and an increased electric field) at moment t_4 . The charge density remaining in the quantum well depends on the duration of the NVP.

In order to obtain an improved picture of the accumulation of dark charge after its depletion by the NVP (the period from t_1 to t_2), we calculated the concentration of charge carriers in the quantum well under a positive bias (Fig. 9). After imposing a positive bias to the well depleted by the NVP, the charge carriers start to accumulate with time, as indicated in Fig. 9 (similar figure describes the hole concentration). Holes accumulate on the n-side interface of the QW, while electrons accumulate on the p-side interface [Fig. 8(b)]. The charging of the structure occurs for 0.1–10 ms (depending on the bias), then the device attains the stationary state and the charge carriers no longer accumulate, as their inflow is balanced by increased recombination.

However, the radiative recombination is negligible and is much too small to be measured experimentally. Moreover, the accumulated charge is insufficient to fully screen

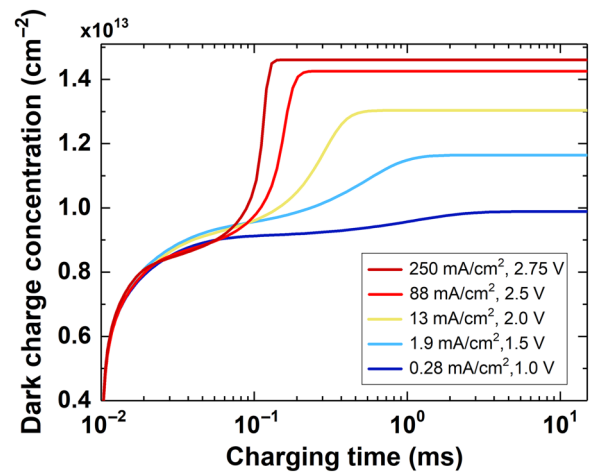


FIG. 9. Concentration of electrons in the quantum well for different dc forward voltages applied to the LED (as indicated in the key). This simulation starts straight after the application of the NVP at moment t_1 . Corresponding current densities (in units of mA/cm^2) are also listed in the key.

the polarization charges (Figs. 7 and 8, moment t_2). Then, if we apply the NVP, this balance is perturbed and the electric field in the QW becomes much weaker. Both accumulated charges then diffuse from the interfaces toward the center of the QW or even the opposite interface, and the radiative recombination becomes much higher. This state does not remain for long, as the charge carriers recombine quickly and their concentrations decay. Figure 9 can be compared with Fig. 6, obtained from Eq. (2). As expected, the gradual increase of dark charge concentration in Fig. 6 is replaced by an accelerated increase in Fig. 9.

In the next step, we calculated the dependence of emission peaks (SPLs) on the charging time before the NVP arrival. The simulation proceeds as follows: the structure is initially set in the depleted-charge state and then the transient simulation starts with a low forward bias imposed, which is not sufficient to turn on the normal LED operation. We are, therefore, in the nonlinear resistance range. After some time, which is varied from 0.1 to 10 ms, an NVP with -10 V is applied for 10 μs , then the forward bias is restored for a short time and the simulation ends. Note that this simulation is different from the experimental procedure since, in the simulation, there is no need for multiple repetitions due to the low sensitivity of the photodetector. Thus, there is only one NVP in every simulation; just the time of charging of the device varies.

The results of this simulation series are presented in Fig. 10, where the intensity of SPL peaks versus charging time is plotted for operating forward voltages between 1 and 2.75 V. In each case, the SPLs increase with charging time until a certain level is reached. Further charging of the device does not result in a noticeable SPL increase. Both the time to reach this state and the SPL intensity

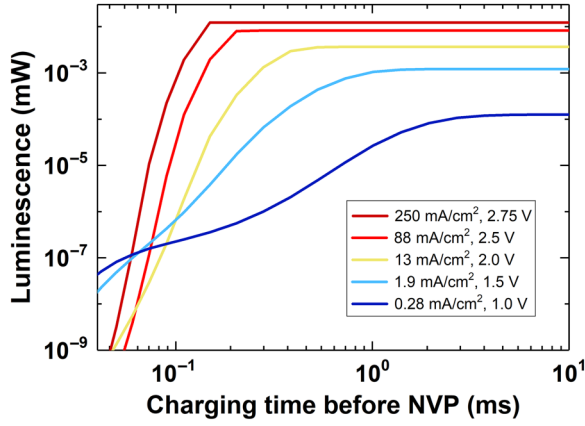


FIG. 10. Simulated intensity of the SPLs (generated by 10- μ s, -10-V NVPs) as a function of charging time before the NVP for various applied forward voltages to the LED (indicated in the key, together with the corresponding current densities in units of mA/cm²).

vary with operating voltage. There is a clear monotonic dependence of both parameters, with a higher operating voltage leading to faster charging time and higher SPL peak intensity. These results agree qualitatively with the experimental results presented in Fig. 2. In the experiment, we are limited by the sensitivity of our detector. As a result, the emission only appears above some threshold level, while in Fig. 10 the emission is always present (though at extremely low levels).

VI. POSSIBILITY OF LASING AT NEGATIVE VOLTAGE

Let us discuss the possibility of achieving lasing during the NVP, assuming that we apply a high reverse bias that fully balances the field in the well (-18 V, according to our simulations). It is important to differentiate between lasing due to a high forward current (which screens the field in most of the well, but dark charge does not contribute to lasing) and lasing happening with a reverse bias and a zero electric field in the well (where all charges accumulated in the well will contribute to lasing). We expect to achieve short (below nanosecond) pulses by switching from positive to negative voltage, which is fairly simple; to generate such short pulses at a positive voltage, one has to apply a special pulse generator. High optical gain can originate from the high concentration of “dark charge” if this charge can be spread evenly across the quantum well by the application of the NVP. Piprek *et al.* have calculated the dependence of material gain of a 25-nm InGaN QW on carrier density that assumes no polarization, i.e., a zero electric field [32]. This, in fact, resembles the conditions during the NVP. The maximal sheet concentration of dark charge that can be accumulated on the ground

state of a wide quantum well will be equal to the polarization charge density at the interfaces if we assume full screening of the polarization field by free carriers. For an In_{0.17}Ga_{0.83}N/GaN well, this polarization charge density equals $1.7 \times 10^{13} \text{ cm}^{-2}$, assuming the constants reported by Bernardini *et al.* [33]. If we now apply a sufficiently large negative voltage, which will eliminate the field in the well, then the dark charge will spread through the whole thickness of the quantum well, leading to an average carrier density of $6.8 \times 10^{18} \text{ cm}^{-3}$. These values can be enhanced by increasing the indium concentration in the well. For example, for an In_{0.22}Ga_{0.78}N/GaN well, we can expect a sheet density of $2.2 \times 10^{13} \text{ cm}^{-2}$ and an average carrier density of $8.8 \times 10^{18} \text{ cm}^{-3}$.

In order to estimate the threshold carrier density n_{th} required for lasing action, we need to consider the optical losses for our laser diodes. The internal losses in the laser diodes strongly depend on the design of the epitaxial structure. Here, we will assume the relatively high internal losses of $\alpha_i = 20 \text{ cm}^{-1}$, which we measured using the Hakki-Paoli technique [34]. The mirror losses for a 1-mm-long resonator without facet coatings are $\alpha_m = 17 \text{ cm}^{-1}$. The modal gain required for the lasing action is, therefore, equal to $G_{\text{th}} = \alpha_i + \alpha_m = 37 \text{ cm}^{-1}$. Piprek *et al.* have also calculated the optical confinement factor for a laser diode with a 25-nm QW to be $\Gamma = 0.097$ [32], which allows us to estimate the threshold material gain as $g_{\text{th}} = G_{\text{th}}/\Gamma = 381 \text{ cm}^{-1}$. The carrier density required to reach such a gain is $9.2 \times 10^{18} \text{ cm}^{-3}$ (Fig. 7 in Ref. [32]), which is higher than the maximum amount that could be supplied from the dark charge. However, for a thinner quantum well of, e.g., 15 nm, the same sheet density of dark charge can give rise to a higher carrier density of $11.3 \times 10^{18} \text{ cm}^{-3}$. For this material density, the gain is equal to a high value of 660 cm^{-1} [32]. For a thinner quantum well, we also need to consider the decrease of the optical confinement factor. We linearly approximate its change with thickness, which gives $\Gamma = 0.0582$ for a 15-nm QW and a threshold material gain of $g_{\text{th}} = 37/0.0582 = 636 \text{ cm}^{-1}$. As can be seen, the material gain (i.e., 660 cm^{-1}) arising from the carriers supplied from the dark charge can be higher than the threshold gain. These are very rough estimates but they show that lasing during the presence of the NVP seems possible.

The threshold material gain can be lowered both by (i) application of high reflectivity dielectric coating on one or both sides of the laser, which can decrease α_m even to 1 cm^{-1} and (ii) reduction of internal losses by optimization of the epitaxial structure designed for a pulsed laser operation with a negative bias.

Our quantum well under a high reverse bias that balances the piezoelectric field, resembles a nonpolar quantum well with a vanishing electric field. Laser diodes grown on nonpolar (m-plane) substrates still suffer from

technological issues, but low threshold current densities have been reported; in Ref. [35], for a m-plane laser diode with three 8-nm In_{0.10}Ga_{0.90}N quantum wells, a threshold current density of 1.54 kA/cm² has been achieved.

To summarize, the possibility of lasing from wide-well structures with NVPs can be improved by (i) increasing the negative voltage, (ii) growing laser diodes with more indium in the well, and (iii) reducing the optical losses.

VII. SUMMARY AND CONCLUSIONS

Electroluminescence from wide-well (In, Ga)N/GaN LEDs can be used to study the slow buildup of dark charge (charge in the ground state) in the well with a low forward current. The concentration of dark charge can be probed by the periodic application of negative voltage pulses (NVPs), which are accompanied by short pulses of light (SPLs). The charging time necessary to observe SPLs depends on the pumping current and the initial concentration of dark charge. This initial concentration depends on the voltage and duration of the NVP. By changing the duration of the NVPs, we can estimate the decay time of the dark charge for different values of negative voltage. Both the charging times at low forward voltage and decay times at negative voltage were in the range of microseconds to milliseconds, orders of magnitude longer than the carrier decay times in narrow wells [19,20] or decay times for the excited states in wide wells [21,24]. The numerical simulations of wide-well LEDs are in qualitative agreement with our electroluminescence results. These studies should help us optimize the laser diode structures with wide wells in order to use NVPs to achieve high population inversion and high gain during SPLs.

ACKNOWLEDGMENTS

This work was partially supported by the National Science Centre Poland within Grants No. 2019/35/D/ST3/03008 and No. 2022/45/B/ST7/03964.

- [1] A. Hangleiter, Jin Seo Im, H. Kollmer, S. Heppel, J. Off, and F. Scholz, The role of piezoelectric fields in GaN-based quantum wells, *MRS Internet J. Nitride Semicond. Res.* **3**, 15 (1998).
- [2] Jin Seo Im, H. Kollmer, J. Off, A. Sohmer, F. Scholz, and A. Hangleiter, Reduction of oscillator strength due to piezoelectric fields in GaN/Al_xGa_{1-x}N quantum wells, *Phys. Rev. B* **57**, R9435 (1998).
- [3] V. Fiorentini, F. Bernardini, F. Della Sala, A. Di Carlo, and P. Lugli, Effects of macroscopic polarization in III-V nitride multiple quantum wells, *Phys. Rev. B* **60**, 8849 (1999).
- [4] T. Takeuchi, S. Sota, M. Katsuragawa, M. Komori, H. Takeuchi, H. Amano, and I. Akasaki, Quantum confined Stark effect due to piezoelectric fields in GaInN strained quantum wells, *Jpn. J. Appl. Phys.* **36**, L382 (1997).
- [5] T. Takeuchi, C. Wetzel, S. Yamaguchi, H. Sakai, H. Amano, and I. Akasaki, Determination of piezoelectric fields in strained GaInN quantum wells using the quantum-confined Stark effect, *Appl. Phys. Lett.* **73**, 1691 (1998).
- [6] H. Turski, M. Chlipala, E. Zdanowicz, E. Rogowicz, G. Muziol, J. Moneta, S. Grzanka, M. Kryśko, M. Syperek, R. Kudrawiec, and C. Skierbiszewski, Competition between built-in polarization and p-n junction field in III-nitride heterostructures, *J. Appl. Phys.* **134**, 243105 (2023).
- [7] M. Leroux, N. Grandjean, M. Laugt, J. Massies, B. Gil, P. Lefebvre, and P. Bigenwald, Quantum confined Stark effect due to built-in internal polarization fields in AlGaIn/GaN quantum wells, *Phys. Rev. B* **58**, R13371 (1998).
- [8] P. Lefebvre, J. Allegre, B. Gil, H. Mathieu, N. Grandjean, M. Leroux, J. Massies, and P. Bigenwald, Time-resolved photoluminescence as a probe of internal electric fields in GaN-GaAlN quantum wells, *Phys. Rev. B* **59**, 15363 (1999).
- [9] F. Della Sala, A. Di Carlo, P. Lugli, F. Bernardini, V. Fiorentini, R. Scholz, and J.-M. Jancu, Free-carrier screening of polarization fields in wurtzite GaN/InGaIn laser structures, *Appl. Phys. Lett.* **74**, 2002 (1999).
- [10] A. Laubsch, W. Bergbauer, M. Sabathil, M. Strassburg, H. Lugauer, M. Peter, T. Meyer, G. Brüderl, J. Wagner, N. Linder, K. Streubel, and B. Hahn, Luminescence properties of thick InGaIn quantum-wells, *Phys. Status Solidi C* **6**, S885 (2009).
- [11] G. Muziol, H. Turski, M. Siekacz, K. Szkudlarek, L. Janicki, M. Baranowski, S. Zolud, R. Kudrawiec, T. Suski, and C. Skierbiszewski, Beyond quantum efficiency limitations originating from the piezoelectric polarization in light-emitting devices, *ACS Photonics* **6**, 1963 (2019).
- [12] G. Muziol, M. Hajdel, M. Siekacz, H. Turski, K. Pieniak, A. Bercha, W. Trzeciakowski, R. Kudrawiec, T. Suski, and C. Skierbiszewski, III-nitride optoelectronic devices containing wide quantum wells—unexpectedly efficient light sources, *Jpn. J. Appl. Phys.* **61**, Sa0801 (2022).
- [13] M. Hajdel, M. Chlipala, M. Siekacz, H. Turski, P. Wolny, K. Nowakowski-Szkudlarek, A. Feduniewicz-Żmuda, C. Skierbiszewski, and G. Muziol, Dependence of InGaIn quantum well thickness on the nature of optical transitions in LEDs, *Materials* **15**, 237 (2022).
- [14] P. Wolny, H. Turski, G. Muziol, M. Sawicka, J. Smalc-Koziorowska, J. Moneta, M. Hajdel, A. Feduniewicz-Żmuda, S. Grzanka, R. Kudrawiec, and C. Skierbiszewski, Impact of interfaces on photoluminescence efficiency of high-indium-content (In, Ga)N quantum wells, *Phys. Rev. Appl.* **19**, 014044 (2023).
- [15] K. Pieniak, W. Trzeciakowski, G. Muziol, A. Kafar, M. Siekacz, C. Skierbiszewski, and T. Suski, Evolution of a dominant light emission mechanism induced by changes of the quantum well width in (In, Ga)N/GaN LEDs and LDs, *Opt. Express* **29**, 40804 (2021).
- [16] G. Muziol, M. Hajdel, M. Siekacz, K. Szkudlarek, S. Stanczyk, H. Turski, and C. Skierbiszewski, Optical properties of III-nitride laser diodes with wide InGaIn quantum wells, *Appl. Phys. Express* **12**, 072003 (2019).
- [17] Z. Zhang, M. Kushimoto, T. Sakai, N. Sugiyama, L. J. Schowalter, C. Sasaoka, and H. Amano, A 271.8 nm deep-ultraviolet laser diode for room temperature operation, *Appl. Phys. Express* **12**, 124003 (2019).

- [18] L. Uhlig, J. Tępaś, M. Hajdel, G. Muziol, and U. T. Schwarz, Transition between quantum confinement and bulklike behavior in polar quantum wells, *Phys. Rev. B* **108**, 045304 (2023).
- [19] U. T. Schwarz, H. Braun, K. Kojima, Y. Kawakami, S. Nagahama, and T. Mukai, Interplay of built-in potential and piezoelectric field on carrier recombination in green light emitting InGaN quantum wells, *Appl. Phys. Lett.* **91**, 123503 (2007).
- [20] V. Simon, M. Wachs, and U. T. Schwarz, Spectral-temporal study on the output power of green InGaN LEDs, *Jpn. J. Appl. Phys.* **58**, SCCC18 (2019).
- [21] J. Tępaś, L. Uhlig, M. Hajdel, G. Muziol, and U. T. Schwarz, Bright emission at reverse bias after trailing edge of driving pulse in wide InGaN quantum wells, *Phys. Status Solidi A* **220**, 2300042 (2023).
- [22] A. Bercha, W. Trzeciakowski, G. Muziol, M. Siekacz, and C. Skierbiszewski, Anomalous photocurrent in wide InGaN quantum wells, *Opt. Express* **28** (4), 4717 (2020).
- [23] A. Bercha, W. Trzeciakowski, G. Muziol, J. W. Tomm, and T. Suski, Evidence for “dark charge” from photoluminescence measurements in wide InGaN quantum wells, *Opt. Express* **31**, 3227 (2023).
- [24] J. W. Tomm, A. Bercha, G. Muziol, J. Piprek, and W. Trzeciakowski, Recombination in polar (In, Ga)N/GaN LED structures with wide quantum wells, *Phys. Status Solidi RRL* **17**, 2300027 (2023).
- [25] A. Bercha, G. Muziol, M. Chlipała, and W. Trzeciakowski, Long-lived excitations in wide (In, Ga)N/GaN quantum wells, *Phys. Rev. Appl.* **20**, 034040 (2023).
- [26] Y. D. Jho, J. S. Yahng, E. Oh, and D. S. Kim, Field-dependent carrier decay dynamics in strained $\text{In}_{1-x}\text{Ga}_x\text{N}$ quantum wells, *Phys. Rev. B* **66**, 035334 (2002).
- [27] Siegfried Selberherr, “*Analysis and Simulation of Semiconductor Devices*” (Springer-Verlag, Wien, 1984).
- [28] P. A. Markowich, C. A. Ringhofer, and C. Schmeiser, “*Semiconductor Equations*” (Springer-Verlag, Wien, 1990).
- [29] Konrad Sakowski, PhD thesis, 2017.
- [30] Maksymilian Dryja, On discontinuous Galerkin methods for elliptic problems with discontinuous coefficients, *Comput. Methods Appl. Math.* **3** (1), 76 (2003).
- [31] K. Sakowski, L. Marcinkowski, P. Strak, P. Kempisty, and S. Krukowski, On the composite discontinuous Galerkin method for simulations of electric properties of semiconductor devices, *Electron. Trans. Numer. Anal.* **51**, 75 (2019).
- [32] J. Piprek, G. Muziol, M. Siekacz, and C. Skierbiszewski, GaN-based bipolar cascade lasers with 25 nm wide quantum wells, *Opt. Quantum Electron.* **54**, 62 (2022).
- [33] F. Bernardini, V. Fiorentini, and D. Vanderbilt, Spontaneous polarization and piezoelectric constants of III–V nitrides, *Phys. Rev. B* **56**, R10024 (1997).
- [34] G. Muziol, H. Turski, M. Siekacz, P. Wolny, S. Grzanka, E. Grzanka, P. Perlin, and C. Skierbiszewski, Enhancement of optical confinement factor by InGaN waveguide in blue laser diodes grown by plasma-assisted molecular beam epitaxy, *Appl. Phys. Express* **8**, 032103 (2015).
- [35] R. M. Farrell, P. S. Hsu, D. A. Haeger, K. Fujito, S. P. DenBaars, J. S. Speck, and S. Nakamura, Low-threshold-current-density AlGaIn-cladding-free m-plane InGaIn/GaN laser diodes, *Appl. Phys. Lett.* **96**, 231113 (2010).